Sedimentary Geology 242 (2011) 34–51

Contents lists available at SciVerse ScienceDirect

Sedimentary Geology

journal homepage: www.elsevier.com/locate/sedgeo

Geological effects and implications of the 2010 tsunami along the central coast of Chile

Robert A. Morton [a], Guy Gelfenbaum [b,*], Mark L. Buckley [c], Bruce M. Richmond [c]

[a] U.S. Geological Survey, 10100 Burnet Rd. Bldg. 130, Austin, TX 78758, USA
[b] U.S. Geological Survey, 345 Middlefield Rd., Menlo Park, CA 94025, USA
[c] U.S. Geological Survey, 400 Natural Bridges Drive, Santa Cruz, CA 95060, USA

ARTICLE INFO

Article history:
Received 21 January 2011
Received in revised form 16 June 2011
Accepted 8 September 2011
Available online 16 September 2011

Editor: G.J. Weltje

Keywords:
Multiple flow directions
Coastal hazards
Sediment transport
Boulders
Sedimentary deposit
Erosion

ABSTRACT

Geological effects of the 2010 Chilean tsunami were quantified at five near-field sites along a 200 km segment of coast located between the two zones of predominant fault slip. Field measurements, including topography, flow depths, flow directions, scour depths, and deposit thicknesses, provide insights into the processes and morphological changes associated with tsunami inundation and return flow. The superposition of downed trees recorded multiple strong onshore and alongshore flows that arrived at different times and from different directions. The most likely explanation for the diverse directions and timing of coastal inundation combines (1) variable fault rupture and asymmetrical slip displacement of the seafloor away from the epicenter with (2) resonant amplification of coastal edge waves. Other possible contributing factors include local interaction of incoming flow and return flow and delayed wave reflection by the southern coast of Peru. Coastal embayments amplified the maximum inundation distances at two sites (2.4 and 2.6 km, respectively). Tsunami vertical erosion included scour and planation of the land surface, inundation scour around the bases of trees, and channel incision from return flow. Sheets and wedges of sand and gravel were deposited at all of the sites. Locally derived boulders up to 1 m in diameter were transported as much as 400 m inland and deposited as fields of dispersed clasts. The presence of lobate bedforms at one site indicates that at least some of the late-stage sediment transport was as bed load and not as suspended load. Most of the tsunami deposits were less than 25 cm thick. Exceptions were thick deposits near open-ocean river mouths where sediment supply was abundant. Human alterations of the land surface at most of the sites provided opportunities to examine some tsunami effects that otherwise would not have been possible, including flow histories, boulder dispersion, and vegetation controls on deposit thickness.

Published by Elsevier B.V.

1. Introduction

Since the 1960 Chilean tsunami, coastal effects of modern tsunamis have been the focus of rapid-response post-event investigations (Miller, 1960; Wright and Mella, 1963; Pflaker et al., 1969; Shi et al., 1993; Gelfenbaum and Jaffe, 2003; Jaffe et al., 2003; Synolakis and Okal, 2005; Goff et al., 2006b; Jaffe et al., 2006). This is because modern tsunamis can provide unequivocal evidence regarding attributes of the waves, characteristics of their deposits, and other criteria used to interpret paleo-tsunami events from the stratigraphic record. Field observations of flow depths, flow directions, and inundation distances from modern tsunamis are also critical for constraining numerical models of inundation and sediment transport and for conducting hazard assessments of populated areas.

The northern, central, and south-central coasts of Chile have a long history of great subduction-zone tsunamigenic earthquakes and those coastal segments are vulnerable to tsunami inundation (Lomnitz, 1970; Lockridge, 1985; Cisternas et al., 2005; Barrientos, 2007). On February 27, 2010, a magnitude 8.8 earthquake offshore from the central coast of Chile (Fig. 1) with a fault-rupture length of approximately 500 km generated a series of waves that inundated the coast for more than 800 km alongshore. Because slip distribution is an important source parameter for generating tsunami waves (Geist and Dmowska, 1999), Delouis et al. (2010), Lay et al. (2010a), Tong et al. (2010), and Lorito et al. (2011) each used inverse modeling to interpret the slip-distribution of the 2010 Chilean earthquake. The models all show the same first-order heterogeneous fault-rupture characteristics, including two patches of slip, one north and one south of the earthquake epicenter, with the northern patch having the greatest displacement. The details of each model are different enough in the magnitude of maximum slip and location of displacement that tsunami model results likely would be different, which underscores the uncertainty associated with detailed earthquake model and tsunami model results. For our purposes the slip results of Delouis et al. (2010) were selected for illustration (Fig. 1) because their inverse modeling utilized both teleseismic and geodetic (GPS,

* Corresponding author. Tel.: +1 6503295483; fax: +1 6503295190.
E-mail address: ggelfenbaum@usgs.gov (G. Gelfenbaum).

0037-0738/$ – see front matter. Published by Elsevier B.V.
doi:10.1016/j.sedgeo.2011.09.004

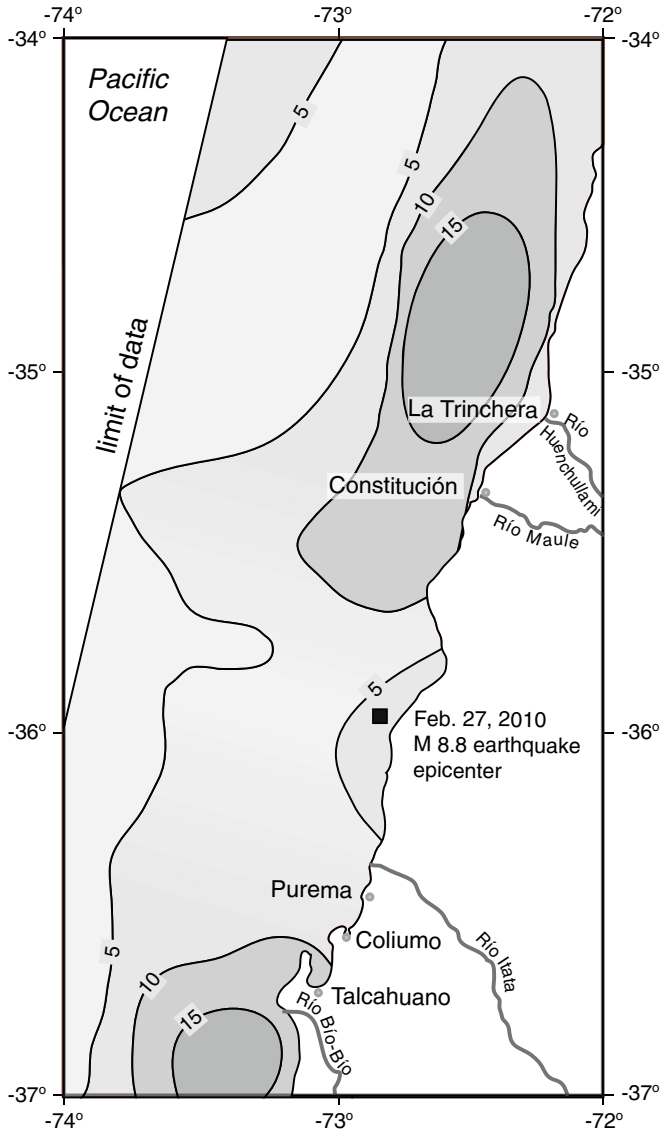

Fig. 1. The central coast of Chile showing locations of the five tsunami study sites, the epicenter of the February 27, 2010 earthquake (filled square), and the complex heterogeneous fault-slip distribution modeled by Delouis et al. (2010). Slip contours are in meters.

InSAR) data sets, and they focused specifically on slip distribution along the fault.

Eyewitnesses of the tsunami generally reported one to four distinct waves with the later waves being the highest and causing the greatest inundation and most destruction (Annunziato et al., 2010; Fritz et al., 2011). The eyewitnesses also consistently reported a lowering of water levels before the highest wave came onshore as a wall of water. Tsunami runup elevations and morphological changes were highly variable over short alongshore distances (Annunziato et al., 2010; Fritz et al., 2011) as a result of alongshore variations in the tsunami wave heights, offshore bathymetry, shoreline orientations, and onshore topography. The highest measured runup elevations typically were associated with steep slopes where beaches were narrow or absent, and lower runup elevations generally were reported where beaches and the adjacent coastal plains were broad and elevations were low.

The region of tsunami inundation exhibits variable shore morphologies consisting of rocky headlands and adjacent arcuate shorelines or embayments with sand beaches that are intersected by rivers with associated alluvial valleys. Most of the coastal towns and villages are built on low-lying coastal plains near the river mouths or on elevated terraces adjacent to the shore. Tidal range in the region is 1.5–2 m. We selected five tsunami-inundation sites for comprehensive investigation along a 200-km segment of coast, extending north and south of the earthquake epicenter between the two patches of maximum fault slip (Fig. 1). The field sites encompassed diverse geological settings including: a coastal plain near a river mouth (La Trinchera), a delta plain (Constitución), two embayed alluvial valleys (Purema and Coliumo), and a combined embayment and delta plain (Talcahuano). All of the sites were selected because their physical settings made them efficient catchments for tsunami deposits and therefore excellent recorders of the 2010 event and potential recorders of past extreme-wave events. Long segments of the central coast of Chile are backed by rocky shores or elevated terraces that have steep nearshore slopes. Detailed observations of tsunami effects were not made at either of these settings because the preservation potential of tsunami deposits is much lower.

Both coseismic uplift and subsidence were reported along the central coast of Chile after the 2010 earthquake. Farías et al. (2010) consistently found evidence of uplift, including exposed wave-cut platforms and marine-algae-encrusted outcrops elevated from 1.5 to 2.0 m along the coast south of Talcahuano. For the coastal segment that included our field study sites, Farías et al. (2010) measured 50 cm of uplift 12 km north of Talcahuano, 15 cm of uplift about 20 km south of Constitución, and 50 cm of subsidence about 20 km north of La Trinchera.

Our study quantifies morphological changes and depositional products of the 2010 Chilean tsunami, examines the influence of vegetation height and density on tsunami deposit thickness, and provides detailed analyses of directions and relative timing of multiple complex onshore and alongshore flows. We believe that the detailed flow-history analyses at Constitución and La Trinchera establish local ground truth that could be used to help constrain tsunami inundation models.

2. Methods

At each of the five study sites, detailed measurements were made of tsunami flow depths, flow directions, vertical erosion, deposit thicknesses, and maximum clast sizes (Table 1). Topographic profiles and inundation distances were surveyed at four of the sites and flow-direction histories were determined at the two open-ocean sites (La Trinchera and Constitución). The field surveys used methods consistent with previous post-tsunami surveys, such as those conducted in Papua New Guinea (Gelfenbaum and Jaffe, 2003), in Peru (Jaffe et al., 2003), in Sri Lanka and Sumatra (Goff et al., 2006b; Jaffe et al., 2006), and in American and Independent Samoa (Richmond et al., 2011a,b).

Because tsunami heights above sea level were measured by other teams (Annunziato et al., 2010; Fritz et al., 2011) we focused our attention on flow depths at each study site. Tsunami flow depths represent the height of the water above the ground surface. Flow-depth measurements have the advantage of not requiring a reference datum (sea level) or correction for tidal stage at the time of the tsunami. Flow speed is also related to flow depth, typically increasing with increasing flow depth. Flow depths were measured on trees in unconfined flow areas to avoid anomalous heights caused by steep slopes. The depths were measured by sighting on a water-level marker (broken tree branches, debris stranded in branches, stripped bark) using a hand-held laser range finder and adding the surveyor's eye height to the recorded height.

Flow directions, looking downstream, were measured with GPS receivers set to magnetic north and later corrected for local magnetic declination. The primary flow-direction indicators were the orientations of bent or broken trees that were still rooted. A few flow directions were obtained from bent shrubs and clumps of grass that were